Unsupervised Segmentation of Hyperspectral Images based on Dominant Edges

Sangwook Lee, Sanghun Lee and Chulhee Lee
Department of Electrical and Electronic Engineering, Yonsei University, 50, Yonsei-ro, Seodaemun-gu, Seoul, Korea

Keywords: Segmentation, Hyperspectral Images, PCA, Dominant Edges.

Abstract: In this paper, we propose a new unsupervised segmentation method for hyperspectral images based on dominant edge information. In the proposed algorithm, we first apply the principal component analysis and select the dominant eigenimages. Then edge operators and the histogram equalizer are applied to the selected eigenimages, which produces edge images. By combining these edge images, we obtain a binary edge image. Morphological operations are then applied to these binary edge image to remove erroneous edges. Experimental results show that the proposed algorithm produced satisfactory results without any user input.

1 INTRODUCTION

Hyperspectral images have been successfully used in many remote sensing applications, which include classifications (Guo, 2006), target detections and environment monitoring (Wang, 2003). In automated processing of remotely sensed images, segmentation is an important first step. With good unsupervised segmentation algorithms, it is generally possible to enhance the performance of many operations (Cao, 2007).

In general, the goal of segmentation is to divide images into their constituent regions. However, in natural scenes, images often contain roads, tree, buildings, fields, ponds, etc. Furthermore, there may be no clear boundaries between the different regions. Consequently, segmentation can be a complex and difficult operation. The segmentation process can be either unsupervised or supervised. Supervised segmentation methods require training data and the application areas of these methods are rather limited. However, unsupervised segmentation methods, which do not require any advanced information, have larger application areas.

Among the various unsupervised segmentation methods, the clustering technique has been most widely used. This technique includes the k-means method and the ISODATA method (Roberts 1997, Meyer 2003). However, it is difficult to apply these methods to hyperspectral images due to prohibitive computational costs and the difficulty of selecting initial points. Furthermore, performance can be rather limited. Efforts have been made to develop segmentation algorithms for hyperspectral images. The morphological method has been proposed to segment hyperspectral images, which use pixel similarities (Pesaresi 2001). A MRF (Markov Random Field) model segmentation method has been proposed, which was based on capturing the intrinsic characteristics of tonal and textural regions (Sarkar 2002). In order to segment hyperspectral images accurately, a number of techniques have been employed, such as mutual information, phase correlation and convex cone analysis (Guo 2006, Erturk 2006, Ifrarraguerri 1999). Statistical segmentation methods have also used a Gaussian mixture model and stochastic estimation maximization (Acito 2000, Masson 1993). Recently, segmentation based on watershed transformation has been proposed (Tarabalka 2010) and Tarabalka et al. proposed a segmentation and classification method using automatically selected markers (Tarabalka 2010).

In this paper, we propose a new unsupervised segmentation method, which is based on edge information and utilizes a post-processing technique to improve segmentation results.

Lee S., Lee S. and Lee C..
Unsupervised Segmentation of Hyperspectral Images based on Dominant Edges.
DOI: 10.5220/0004739705880592
In *Proceedings of the 9th International Conference on Computer Vision Theory and Applications* (VISAPP-2014), pages 588-592
ISBN: 978-989-758-003-1

2 SEGMENTATION USING EDGE FUSION AND REGION GROWING

Fig. 1 shows a block diagram of the proposed method. First, we apply the principal component analysis using the method described in (Lim S, 2001) and select the dominant eigenimages. Then edge operators are applied to find the edge pixels. This procedure is repeated for each of the retained dominant eigenimages and the edge images are then combined to produce a reference edge image. Finally, we apply morphological operations and post-processing to improve the segmentation results.

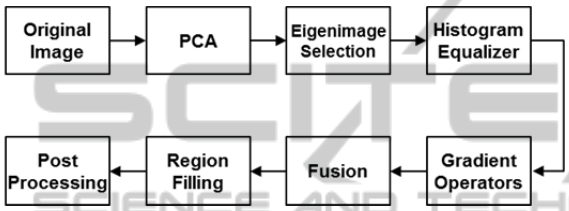

Figure 1: Block diagram of the proposed method.

2.1 Gradient Operators

Fig. 2 shows some eigenimages. The first three eigenimages corresponding to the largest eigenvalues retained about 99% of the total energy, which is the squared sum of all the pixels. In the proposed method, we applied an edge detection algorithm and histogram equalizer to the three eigenimages after performance evaluation on the number of eigenimages. To acquire the edges of eigenimages, we applied gradient operators as follows:

$$S_i(m,n) = EG_i(m,n) * Sb(m,n)$$
$$R_i(m,n) = EG_i(m,n) * Rb(m,n) \quad (1)$$

where $EG_i(m,n)$ is the i-th eigenimage and $Sb(m,n)$ and $Rb(m,n)$ are the Sobel operator and the Robinson operator. $S_i(m,n)$ and $R_i(m,n)$ are the i-th the Sobel and the Robinson edge image. Mainly horizontal and vertical edge components are produced by the Sobel filter and diagonal edge components are acquired by the Robison filter. We applied this procedure to the selected eigenimages and obtained the corresponding edge images. Therefore, 6 edge images were produced. Fig. 3 shows the edge images.

Then we applied the threshold operation to the edge images and obtained binary edge images. The threshold value was computed from the mean and variance of the edge image as follows:

$$Threshold = \mu - k\sigma \quad (2)$$

where μ and σ represent the mean and standard deviation values, which were calculated from the edge images. In (2), k is a coefficient, which we set to 0.35, which was chosen empirically after testing different coefficients. To combine the edge images, we computed the union and intersection edge images and the reference binary edge image are produced as follows:

$$E(m,n) = EI_1(m,n) \cup EI_2(m,n) \ldots \cup EI_n(m,n) \quad (3)$$

where $EI_j(m,n)$ is the *j-th* edge image and $E(m,n)$ is the reference binary edge image (Fig. 4).

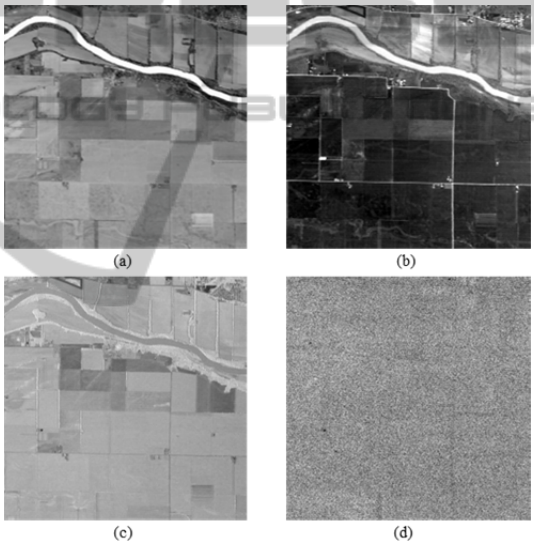

Figure 2: The eigenimages (a) the 1st eigenimage, (b) the 3rd eigenimage, (c) the 5th eigenimage and (d) the 7th eigenimage.

2.2 Morphological Operations and Post Processing

We can view the edges of the reference binary edge images as boundaries between regions. The reference binary edge image contains a number of regions (connected components), which can be found using a connected component labeling algorithm. However, some of the connected components may be small. We select the connected components whose sizes are larger than a threshold value. In this paper, we empirically set the threshold value as 22. Connected components may contain

many small holes. To eliminate these holes, we apply a region filling method. Fig. 5(b) shows the output image after the region filling method was applied.

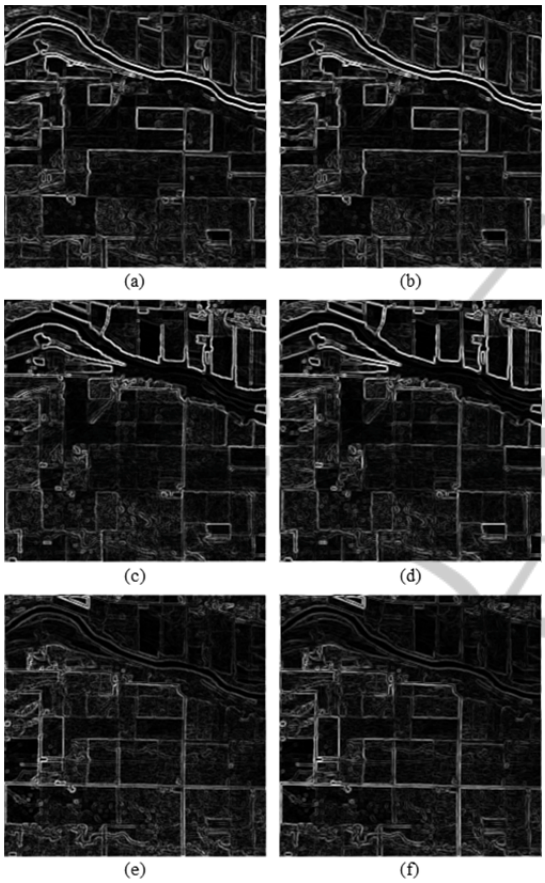

Figure 3: The edge images of the selected eigenimages (a) the Sobel edge image of the 1st eigenimage, (b) the Sobel edge image of the 2nd eigenimage, (c) the Sobel edge image of the 3rd eigenimage, (d) the Robinson edge image of the 1st eigenimage, (e) the Robinson edge image of the 2nd eigenimage and (f) the Robinson edge image of the 3rd eigenimage.

Pixels at boundaries may generally be unclassified even after performing the region filling procedure, even if they belong to a region. In order to assign these kinds of pixels to one of the identified regions, we compute the mean vector and covariance matrix of each region (connected component). Assuming that each region could be approximated by a normal distribution, for each unclassified pixel within 5 pixels from the boundary pixels, we compute the following *chi*-square distribution:

$$y_i(x) = (x - m_i)^t \Sigma_i^{-1} (x - m_i) \quad (4)$$

where x represents an unclassified pixel, m_i represents the mean vector of the *i-th* region and Σ_i represents the covariance matrix of the *i-th* region. If $y_i(x)$ is smaller than the threshold value and $y_i(x) < y_j(x)$, we assign the pixel to the *i-th* region where j refers to all neighbour connected components other than the *i-th* region. Fig. 5(c) shows the final segmented image after post-processing.

Figure 4: Reference binary edge image.

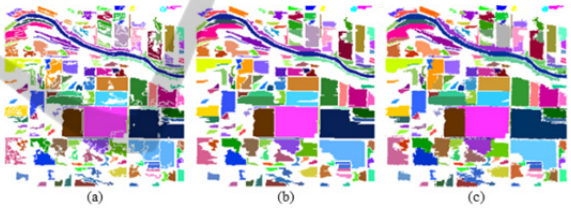

Figure 5: (a) An image before region growing, (b) an image after region fills, and (c) the segmented image after post processing.

3 EXPERIMENTAL RESULTS

We evaluated the performance of the proposed algorithm using the AVIRIS (Airborne Visible/Infrared Imaging Spectrometer) over some agricultural areas. There are 220spectral bands in the 0.4 to 2.4 μm regions. This data set contains 2166 scan lines with 614 pixels in each scan line. From the data set, we selected a sub-region of 613 × 613 pixels.

The proposed method produced a good segmentation result although it is completely automated. Most fields were correctly identified with clear boundaries. Next, the proposed algorithm was compared with the k-means algorithm. In order to apply the k-means method, the spectral bands of the original hyperspectral image were reduced by averaging the four adjacent spectral bands. The

averaging procedure would eliminate the noise factors of the spectral bands. The segmentation results of the two methods are shown in Fig. 6. The proposed method produced a much better result than the k-means method. The proposed method was also faster than the k-means method by 4.29 times in terms of processing time.

Table 1: Information of reconstruction images when using the proposed algorithm.

Group	Field	Area	Correct (%)	Incorrect (%)	No. detect (%)
1	Tree	168	0.0%	0.0	100.0
2	Corn1	578	99.7	0.0	0.3
3	Water	80	100.0	0.0	0.0
4	Pasture1	360	99.2	0.0	0.8
5	Corn2	360	14.2	0.0	85.8
6	Corn3	416	62.0	0.0	38.0
7	Pasture2	333	95.5	0.0	4.5
8	Corn4	792	97.3	0.0	2.7
9	Wheat	774	99.7	0.0	0.3
10	Soy1	792	96.8	0.0	3.2
11	Corn5	684	82.3	0.0	17.7
12	Corn6	1107	88.6	0.0	11.4
13	Soy2	1400	99.5	0.0	0.5
14	Corn7	1800	99.7	0.0	0.3
15	Corn8	540	81.5	0.6	18.0
16	Soy3	450	96.7	0.0	3.3
17	Corn9	480	97.9	0.0	2.1
18	Soy4	324	50.3	0.0	49.7
19	Soy5	1482	99.8	0.0	0.2
20	Soy6	594	99.8	0.0	0.2
21	Soy7	952	43.9	10.2	45.9
Total	-	14466	81.1638	0.5116	18.3245

In order to provide quantitative analyses, we selected 12 classes from the AVIRIS data, as shown in Fig. 6(a). Table 1 shows the class description. It also shows the percentile of correctly classified pixels and incorrectly classified pixels. The proposed method produced a much better result than the k-means method (Table 2). It is noted that the proposed method may produce a number of unclassified pixels.

4 CONCLUSIONS

In this paper, we have proposed a completely automated segmentation method. The key idea of the proposed method is to use the edge information of the dominant eigenimages. Although the proposed method is unsupervised and does not require any

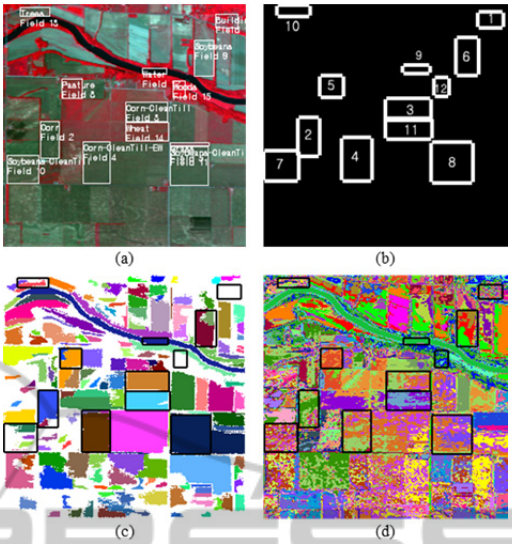

Figure 6: Performance comparisons: (a) the truth map, (b) number of regions (c) the result of the proposed algorithm, and (d) the result of the k-means algorithm.

Table 2: Information of reconstruction images when using the k-means algorithm.

Group	Field	Area	Correct (%)	Incorrect (%)	No. detect (%)
1	Tree	168	21.4	78.6	0
2	Corn1	578	41.7	58.3	0
3	Water	80	100	0	0
4	Pasture1	360	66.9	33.1	0
5	Corn2	360	24.2	75.8	0
6	Corn3	416	48.0	51.92	0
7	Pasture2	333	61	39	0
8	Corn4	792	42.1	57.9	0
9	Wheat	774	56.7	43.3	0
10	Soy1	792	39.8	60.2	0
11	Corn5	684	37.7	62.3	0
12	Corn6	1107	44.8	55.2	0
13	Soy2	1400	62.4	37.6	0
14	Corn7	1800	55	45	0
15	Corn8	540	41.3	58.7	0
16	Soy3	450	52.7	47.3	0
17	Corn9	480	78.6	21.4	0
18	Soy4	324	66.8	33.2	0
19	Soy5	1482	41.1	58.9	0
20	Soy6	594	40.6	59.4	0
21	Soy7	952	35	65	0
Total	-	14466	50.5	49.5	0

user intervention, it can provide fairly good segmentation results. The proposed algorithm is relatively simple and easy to implement, and it

compares favourably with existing unsupervised methods.

REFERENCES

Acito N, Corsini G and Diani M 2000. An unsupervised algorithm for hyperspectral image segmentation based on the Gaussian mixture model. *in Proc, IGARSS*, pp. 3745-3747.

Cao F, Hong W, Wu Y and Pottier E 2007. An Unsupervised Segmentation With an Adaptive Number of Clusters Using the SPAN/H/α/A Space and the Complex Wishart Clustering for Fully Polarimetric SAR Data Analysis. *IEEE Trans., Geosci. Remote Sens.*, vol. 45, no.11, pp. 3454-3467.

Erturk A and Erturk S 2006 . Unsupervised Segmentation of Hyperspectral Images Using Modified Phase Correlation. *IEEE Geosci. Remote Sens. Lett.*, vol. 3, no. 4, pp. 527-531.

Guo B. Gunn S. R. and Damper R. I. 2006. Band Selection for Hyperspectral Image Classification Using Mutual Information. *IEEE Geosci. Remote Sens. Lett.*, vol. 3, no. 4, pp. 522-526.

Ifrarraguerri A and Chang C. I. 1999. Multispectral and hyperspectral image analysis with convex cones. *IEEE Trans., Geosci. Remote Sens.*, vol. 37, no. 2, pp. 756 – 770.

Lim S, Sohn K and Lee C 2001. Principal Component Analysis for Compression of Hyperspectral Images. *Proc. IEEE IGARSS*, vol. 1, pp. 97-99.

Masson P and Pieczynski W 1993. SEM algorithm and unsupervised statistical segmentation of satellite images. *IEEE Trans., Geosci, and Remote Sens.*, vol. 31, no. 3, pp. 618– 633.

Meyer A, Paglieroni D and Astaneh C 2003. K-means re-clustering: Algorithmic options with quantifiable performance comparisons. *Proceedings of the SPIE, Volume 5001*, pp. 84-92.

Pesaresi M and Benediktsson A 2001. A New Approach for the Morphological Segmentation of High-Resolution Satellite Imagery. *IEEE Trans., Geosci. Remote Sens.*, vol. 39, no. 2, pp. 309-320.

Robert AS 1997. *Remote sensing: models and methods for image processing*. Academic Press, 2nd edit., pp. 389-447.

Sarkar A, Biswas M. K. and Kartikeyan B 2002. A MRF Model-Based segmentation Approach to classification for Multispectral imagery. *IEEE Trans., Geosci. Remote Sens.*, vol. 40, no. 5, pp. 1102-1113.

Tarabalka Y, Chanussot J, and Benediktsson J. A. 2010. Segmentation and Classification of Hyperspectral Images Using Minimum Spanning Forest Grown From Automatically Selected Markers. *IEEE Trans. Systems, Man, and Cybernetics—PART B: Cybernetics*, vol. 40, no. 5, pp. 1267 – 1279.

Tarabalka Y, Chanussota J, and Benediktsson JA 2010. Segmentation and classification of hyperspectral images using watershed transformation. *Pattern Recognition*, vol. 43, Iss. 7, pp. 2367–2379.

Wang S, Yan F, Zhu L, Wang L and Jiao Y 2003. Water quality monitoring using hyperspectral remote sensing data in Taihu Lake China. *Proc., IGARSS*, pp. 4553-4556.